

Supporting Information

**Room-Temperature Half-Metals Induced by Chemical Surface Modification: 2D
 Mn_2Se_2 monolayer**

Zhe Wang, Yanqiu Zheng, Ji Chen, Yun Wang, Yu Liang, Xiang Li, Fang Wu*

College of Information Science and Technology, Nanjing Forestry University, Nanjing, Jiangsu
210037, P. R. China

E-mail: fangwu@njfu.edu.cn

Table S1. Optimized lattice parameters a and b (\AA), magnetic moment $M(\mu_B)$ of the Mn atom, energy difference (per Mn atom) between the FM and AFM states $\Delta E = E_{\text{FM}} - E_{\text{AFM}}$ (meV) for Mn_2Se_2 calculated using the GGA+U method with different U values. The available experimental data are listed in parentheses for comparison.

| U (eV) | a, b(\AA) | M(μ_B)/Mn | ΔE(meV) |
|---------------|--------------------------------------|---------------------------------|-----------------------------------|
| 1 | 4.207 | ± 4.160 | 351 |
| 2 | 4.264 | ± 4.345 | 258 |
| 2.3 | 4.282 (4.28) | $\pm 4.386 (\pm 4.38)$ | 236(232) |
| 2.5 | 4.291 | ± 4.410 | 221 |
| 3 | 4.309 | ± 4.461 | 189 |
| 4 | 4.347 | ± 4.546 | 155 |
| 5 | 4.375 | ± 4.609 | 113 |

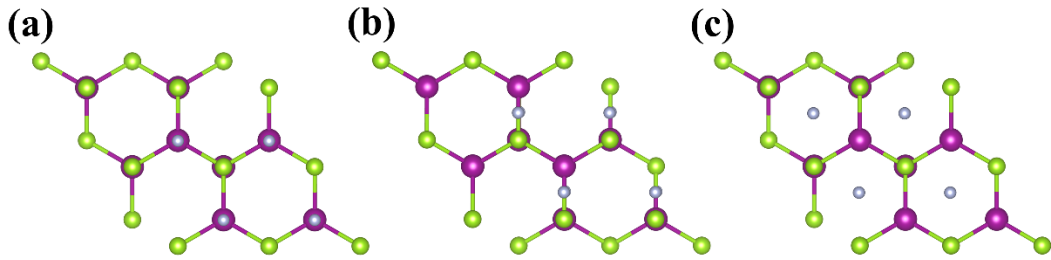


Figure S1. Schematic structures of Mn_2Se_2 monolayers modified with X atoms (X=F, Cl, Br, I and S) at the several adsorption sites (a) on-top, (b) bridge, (c) hollow. The purple, green, and gray balls represent Mn, Se, and X atoms, respectively.

Table S2. The total energies (in eV) of Mn_2Se_2 monolayer with F, Cl, Br, I and S adsorption at different adsorption sites (i.e. on-top, bridge and hollow sites).

| adsorption sites | on-top | bridge | hollow |
|---|---------------|---------------|---------------|
| $\text{Mn}_2\text{Se}_2\text{F}_2$ | -144.632 | -144.388 | -144.486 |
| $\text{Mn}_2\text{Se}_2\text{Cl}_2$ | -132.804 | -132.548 | -132.664 |
| $\text{Mn}_2\text{Se}_2\text{Br}_2$ | -128.816 | -128.601 | -128.716 |
| $\text{Mn}_2\text{Se}_2\text{I}_2$ | -124.936 | -124.432 | -123.992 |
| $\text{Mn}_2\text{Se}_2\text{S}_2$ | -137.248 | -136.776 | -136.410 |

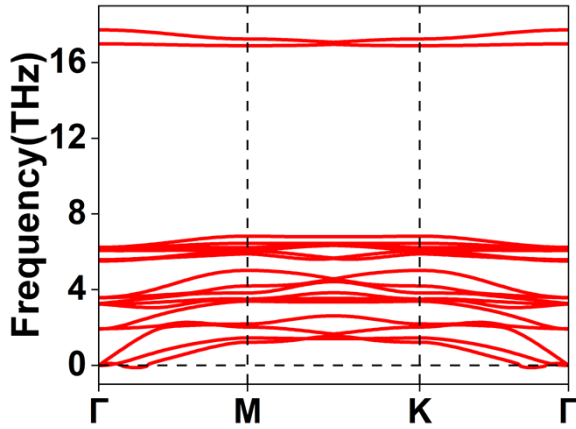


Figure S2. Phonon dispersion curves of $\text{Mn}_2\text{Se}_2\text{F}_2$ monolayer.

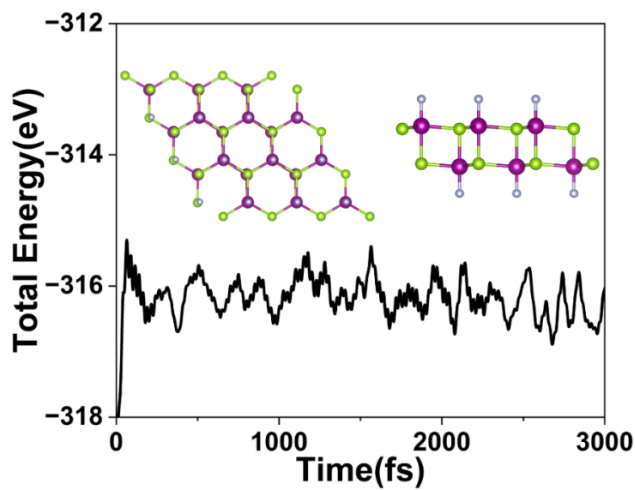


Figure S3. Evolution of total energy for the $\text{Mn}_2\text{Se}_2\text{F}_2$ monolayer at 300 K from AIMD simulations. Here, top views and side views of the corresponding geometrical structures after the AIMD simulation are shown.

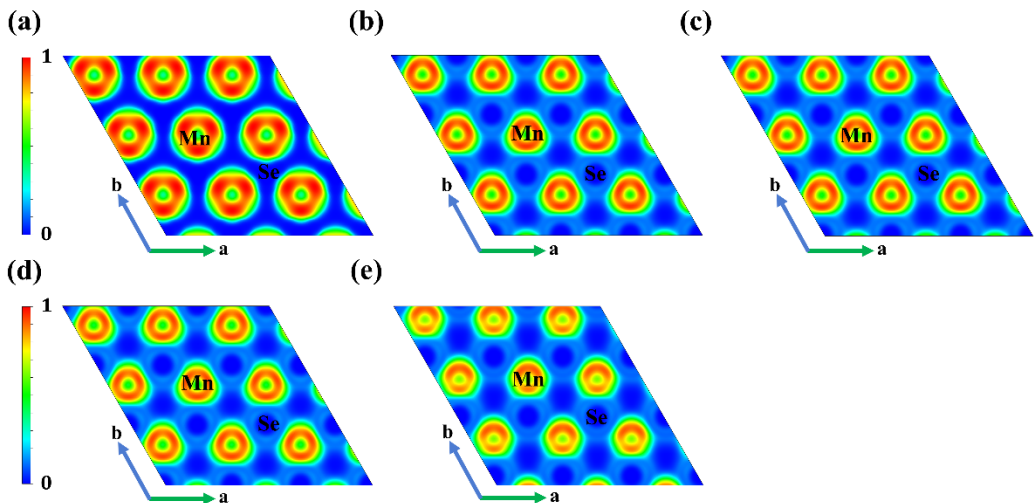


Figure S4. Electron localization functions (ELF) of (a) $\text{Mn}_2\text{Se}_2\text{F}_2$, (b) $\text{Mn}_2\text{Se}_2\text{Cl}_2$, (c) $\text{Mn}_2\text{Se}_2\text{Br}_2$, (d) $\text{Mn}_2\text{Se}_2\text{I}_2$ and (e) $\text{Mn}_2\text{Se}_2\text{S}_2$ monolayers.

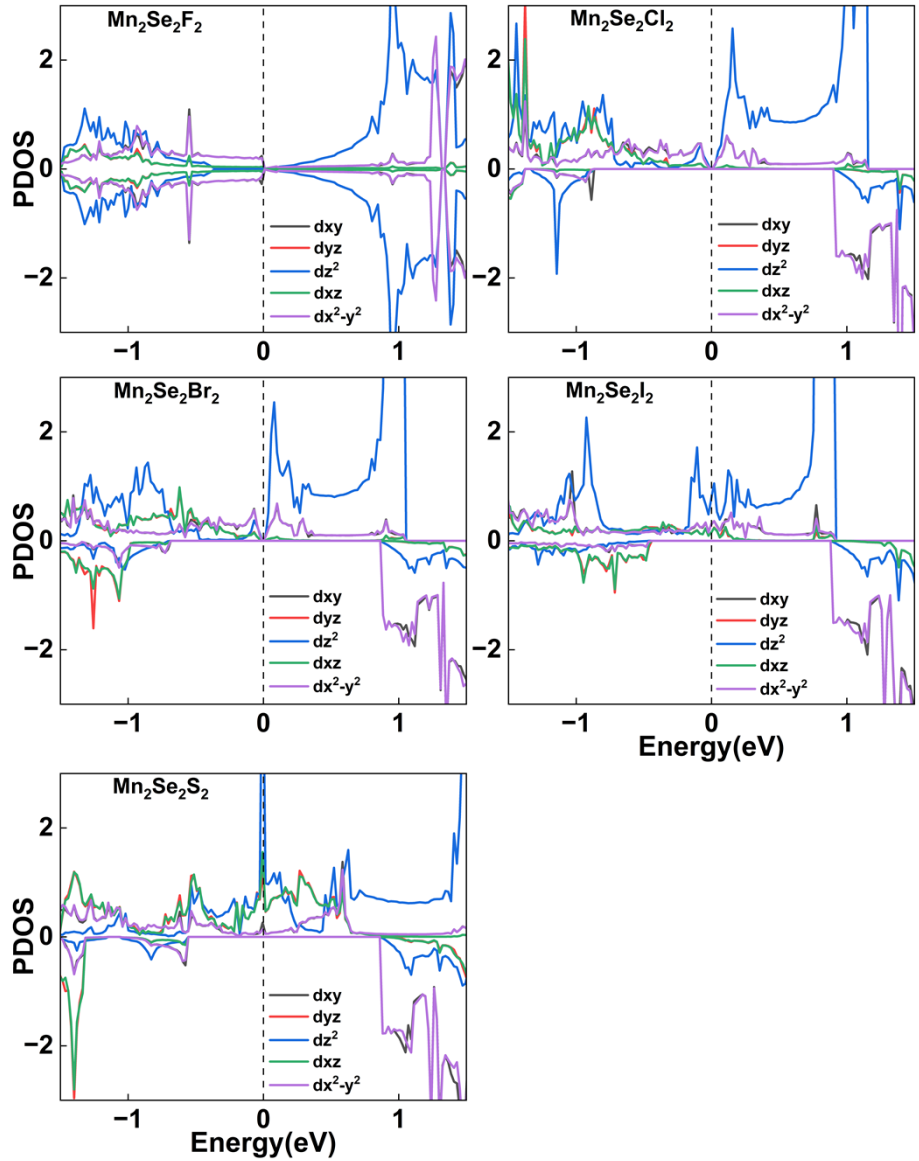


Figure S5. The PDOS of Mn d orbitals for Mn_2Se_2 derivatives monolayer.